



Synergistic protection of quercetin and lycopene against oxidative stress via SIRT1-Nox4-ROS axis in HUVEC cells

Xuan Chen^a, Liufeng Zheng^a, Bing Zhang^a, Zeyuan Deng^{a,b,**}, Hongyan Li^{a,*}

^a State Key Laboratory of Food Science and Technology, Nanchang University, Nanchang, 330047, Jiangxi, China

^b Institute for Advanced Study, Nanchang University, Nanchang, 330031, Jiangxi, China

ARTICLE INFO

Keywords:

Reactive oxygen species
Quercetin
Lycopene
SIRT1
NADPH oxidase 4
Endothelial protection

ABSTRACT

Oxidative stress is a potential factor in the promotion of endothelial dysfunction. In this research, flavonoids (quercetin, luteolin) combined with carotenoids (lycopene, lutein), especially quercetin-lycopene combination (molar ratio 5:1), prevented the oxidative stress in HUVEC cells by reducing the reactive oxygen species (ROS) and suppressing the expression of NADPH oxidase 4 (Nox4), a major source of ROS production. RNA-seq analysis indicated quercetin-lycopene combination downregulated inflammatory genes induced by H₂O₂, such as IL-17 and NF-κB. The expression of NF-κB p65 was activated by H₂O₂ but inhibited by the quercetin-lycopene combination. Moreover, the quercetin and lycopene combination promoted the thermostability of Sirtuin 1 (SIRT1) and activated SIRT1 deacetyl activity. SIRT1 inhibitor EX-527 attenuated the inhibitory effects of quercetin, lycopene, and their combination on the expression of p65, Nox4 enzyme, and ROS. Quercetin-lycopene combination could interact with SIRT1 to inhibit Nox4 and prevent endothelial oxidative stress, potentially contributing to the prevention of cardiovascular disease.

1. Introduction

Endothelial dysfunction, which refers to a series of changes that occur in endothelial cells when exposed to stress factors, including increased permeability and decreased integrity, is an important contributor to the pathobiology of atherosclerotic cardiovascular disease (CVD) (Goligorsky, 2005; Seals et al., 2011). Among the stress factors, oxidative stress is considered a key factor of CVD and regulator of endothelial dysfunction in aging, inflammation, and atherosclerosis (Santilli, D'Ardes and Davi, 2015). Oxidative stress often results from the excessive accumulation of reactive oxygen species (ROS) and redox imbalance (Devasagayam et al., 2004). Amelioration of ROS-dependent endothelial dysfunction is critical to retard the development of CVDs (Lassègue and Griendling, 2010). Many researchers focused on improving antioxidant efficiency through activating antioxidant-related signaling cascades, enzymes, and inherent antioxidants to mitigate oxidative stress, however, few were focused on the suppression of ROS production (Yu et al., 2019; Zhang and Tsao, 2016). A burst of ROS production, with the activation of ROS formation systems such as Nicotinamide adenine dinucleotide phosphate (NADPH) oxidase, is

critical to the development of CVDs (D'Oria et al., 2020). Thus, strategies that inhibit ROS production are promising for improving CVD outcomes.

Sirtuins, a class III nicotinamide adenine dinucleotide- (NAD-) dependent histone deacetylase, owns seven members in mammals (SIRT1-7). Among them, silent mating type information regulation 2 homolog 1 (SIRT1) is a very important member and plays a critical role in metabolic syndromes, oxidative stress, inflammation, and aging (Yu and Auwerx, 2010; Zhang et al., 2017). It plays a key role in regulating endothelial functions and CVDs (Potente et al., 2007). The cardioprotective role of SIRT1 was related to the regulation of several pathways, such as SIRT1/FOXOs, SIRT1/NF-κB, SIRT1/Nox, SIRT1/SOD, and SIRT1/eNOs (Zhang et al., 2017). NADPH oxidase isoforms (Noxs) family is a major source of ROS generation, among which Nox4 was highly expressed in cardiovascular tissues (Chen et al., 2012). SIRT1 promoted antioxidant enzyme activity and restored ROS-mediated oxidative injuries by decreasing Noxs activity (Zhang et al., 2016), suggesting that SIRT1 may be an upstream regulator of Noxs in HUVECs (Schilder et al., 2009). This evidence indicated the Nox4 suppressive role of SIRT1 in endothelial dysfunction. However, whether SIRT1

* Corresponding author.

** Corresponding author. State Key Laboratory of Food Science and Technology, Nanchang University, Nanchang, 330047, Jiangxi, China.

E-mail addresses: dengzy@ncu.edu.cn (Z. Deng), lihongyan@ncu.edu.cn (H. Li).

<https://doi.org/10.1016/j.crfs.2022.10.018>

Received 11 July 2022; Received in revised form 26 September 2022; Accepted 14 October 2022

Available online 18 October 2022

2665-9271/© 2022 The Authors. Published by Elsevier B.V. This is an open access article under the CC BY-NC-ND license (<http://creativecommons.org/licenses/by-nc-nd/4.0/>).

regulates oxidative stress in CVDs in a Nox4-dependent way remains unclear.

Plant-derived antioxidants such as flavonoids (quercetin, luteolin) and carotenoids (lycopene, lutein) were reported to improve endothelial function, which was correlated with the prevention of oxidative stress (Chen et al., 2020; Chen et al., 2021c; Hung et al., 2015; Kim et al., 2011). They could increase the expression of SIRT1 to prevent endothelial dysfunction, aging, and metabolic diseases (Balcerzyk et al., 2014; Hung et al., 2015; Luvizotto et al., 2015; Xiao et al., 2014). Flavonoids and carotenoids usually co-existed in fruits and vegetables, such as watermelon, sweet pepper, citrus fruits, and leafy green vegetables (Kaulmann et al., 2016; Pan et al., 2018; Shang et al., 2022; Sinisgalli et al., 2020). Their interactive health effects on fruits and vegetables were reported (Phan et al., 2019; Sinisgalli et al., 2020). The combination of phenolic acids and β -carotene synergistically prevented H₂O₂-induced oxidative stress by regulating the Nrf2-Keap1 signaling pathway in H9c2 cells (Pan et al., 2021). The combinations of petunidin and lycopene showed synergistic cardioprotective effects through altering Nrf2 and PI3K-Akt cascades (Zheng et al., 2020). Previously, we reported that there were synergistic or antagonistic effects of flavonoids (quercetin, luteolin) and carotenoids (lycopene, lutein) on antioxidant activity (Chen et al., 2021a). However, their mechanism of synergistic antioxidant activity remains unclear. Plant-derived antioxidants reduced ROS levels through activating antioxidant systems (*in vivo* enzymes, antioxidants such as glutathione) or directly scavenging ROS. However, whether they could synergistically suppress Nox4 to inhibit ROS production and the possible cardioprotective effects is not fully understood.

We hypothesized that flavonoid-carotenoid combinations mitigate oxidative stress by regulating SIRT1 in the Nox-dependent pathway, which plays a critical role in cardiac protection. To test this hypothesis, human umbilical vein endothelial cells (HUVECs) were exposed to H₂O₂ to induce oxidative stress, and the role of flavonoid-carotenoid combinations in regulating SIRT1 and ROS production was detected in this research.

2. Material and methods

2.1. Chemicals and reagents

Hydrogen peroxide (H₂O₂) solution (30 wt % in H₂O), quercetin, luteolin, lutein, and lycopene (purity $\geq 99\%$) were purchased from Shanghai Aladdin Reagents Co. (Shanghai, China). Ham's F-12K (Kaighn's) Medium (F-12K) was purchased from Procell Life Science & Technology Co., Ltd. (Wuhan, China). Anti-Nox4 antibody ab 133,303, anti-NF- κ B p65 antibody ab32536 were obtained from Abcam Ltd. (Cambridge, UK), phospho-NF- κ B p65 (Ser536) (93H1) Rabbit mAb 3033 were purchased from Cell Signaling Technology, Inc. (Massachusetts, United States). Anti- β -actin HC201-01 was obtained from TransGen Biotech Co. (Beijing, China). Secondary antibodies horseradish peroxidase-conjugated anti-rabbit (L3012) or anti-mouse (L3032) were purchased from Signalway Antibody (Nanjing, China). 2', 7'-Dichlorodihydrofluorescein diacetate (DCFH-DA) were purchased from Sigma-Aldrich ((St. Louis, MO, USA). CCK-8 assay kit, nuclear extraction kit, and RIPA lysis buffer, super-enhanced chemiluminescence detection reagent were purchased from the Beyotime Institute of Biotechnology (Shanghai, China). HUVEC cell line was obtained from Procell Life Science & Technology Co., Ltd. (Wuhan, China). Recombinant-SIRT1 protein was purchased from Proteintech Group, Inc. (Wuhan, China).

2.2. Cell culture and cell viability

HUVEC cells were cultured in F-12K medium containing 10% (v/v) FBS, and 1% penicillin/streptomycin were added to the medium. Cells were incubated at 37 °C in a humidified incubator with 95% air and 5% CO₂. Cell viability was determined by the CCK-8 assay, which is a cell

proliferation assay using WST-8 cleavage. In brief, HUVEC cells (1×10^5 cells per well) were plated into a 96-well plate and reached 90% confluence before treatments. A total of 1500 μ M H₂O₂ was used to induce around 50% oxidative damage in HUVEC cells (Chen et al., 2021a). After various pre-treatment, cells were then reacted with 10% CCK-8 for 1 h. Moreover, 0.1% DMSO or THF was added to the control groups. Absorbance was recorded at 450 nm using a microplate reader (Thermo Scientific Varioskan Flash, Vantaa, Finland). Cell viability (%) = [A(sample) - A (background)]/[A (control) - A (background)] \times 100.

2.3. ROS detection

2.3.1. Flow-cytometry

Quercetin and luteolin were dissolved in dimethyl sulfoxide (DMSO), lutein and lycopene were dissolved in tetrahydrofuran (THF, Damao Co. Ltd., Tianjin, China) at a concentration of 10 mM, respectively, and then freshly diluted in culture medium with 5% fetal bovine serum (FBS). The final concentration of DMSO and THF in culture medium was below 0.1% (v/v) and 0.05% (v/v), respectively. HUVEC cells were plated into 12-well plates at a density of 1×10^5 cells per well and reached 90% confluence, then treated with 8 μ M individual or combined phytochemicals for 12 h, and induced by H₂O₂ for 1 h, followed by incubation with 30 μ M DCFH-DA in the medium at 37 °C for 20 min in darkness. After centrifugation at 1500 rpm for 5 min, the supernatants were removed, and resuspended in PBS. Fluorescence was measured by flow cytometry (BD biosciences). Data were processed using FlowJo software Version 7.6.1 (BD Life Sciences, USA).

2.3.2. High content screening

HUVEC cells were plated in CellCarrier-96 Ultra microplate to reach confluency. After various treatments, cells were washed twice with PBS and incubated 30 μ M DCF-DA for 30 min at 37 °C in darkness. After washing with serum-free F-12K in the dark, the level of ROS was measured by using a high content analysis (HCA) system and data analysis with Harmony 4.9.

2.4. RT-qPCR analysis

Cell total RNA was extracted using Trizol reagent (Invitrogen) according to the manufacturer's instructions, and quantified by a NanoDrop ND-1000 spectrophotometer. A total of 1 μ g of RNA was reverse-transcribed into cDNA using a Prime Script RT reagent kit (Takara, Otsu, Japan). The cDNA was then mixed with SYBR Green Supermix (DBI bioscience, German) and the primers (Table S1) for RT-qPCR analysis. The relative gene expression was adjusted with β -actin using the $2^{-\Delta\Delta CT}$ method and normalized to that of the control group.

2.5. Western-Blot analysis

Cell extracts were separated by 10% sodium dodecyl sulphate-polyacrylamide gel electrophoresis (SDS-PAGE), and transferred to polyvinylidene fluoride (PVDF) membranes (Roche Diagnostics GmbH, Mannheim, Germany). The membrane was blocked in 5% skim milk for 2 h and incubated with primary antibodies overnight at 4 °C. PVDF membranes were washed with TBST and incubated with secondary antibodies for 2 h at room temperature and visualized by ECL reagent and detected using the enhanced chemiluminescence detection system (Image Lab™ Touch Software, BIO-RAD, USA). An image analyzer (ImageLab, BIO-RAD, USA) was used to determine the band intensity, and the relative expression of proteins was normalized to β -actin.

2.6. RNA-sequencing analysis

Isolated RNA with Trizol reagent (Invitrogen) was used for RNA-seq analysis subsequently. RNA-seq library construction and sequencing were performed using the BGISEQ-500 platform. The clean reads were

mapped to the reference genome using HISAT2 (v2.0.4) (Kim et al., 2015). Bowtie2 (v2.2.5) (Langmead and Salzberg, 2012) was applied to align the clean reads to the reference coding gene set, then the expression level of gene was calculated by RSEM (v1.2.12) (Li and Dewey, 2011). The heatmap was drawn by pheatmap (v1.0.8) according to the gene expression in different samples. Genes with ≥ 2 -fold change and false discovery rates (FDR) ≤ 0.001 were considered as statistically significant. Differential expression analysis was performed using the DESeq2 (v1.4.5) with Q value ≤ 0.05 . The Gene Ontology (GO) enrichment analysis (<http://www.geneontology.org/>) and Kyoto Encyclopedia of Genes and Genomes (KEGG) (<https://www.kegg.jp/>) enrichment analysis of annotated different expressed genes was performed by Phyper (https://en.wikipedia.org/wiki/Hypergeometric_distribution) based on Hypergeometric test.

2.7. Cellular thermal shift assay

Cellular thermal shift assay (CETSA) was conducted according to Jafari et al. (Jafari et al., 2014) with minor adjustments. A total of 1.0×10^6 HUVEC cells were cultured in 10 cm dishes to reach 100% confluency before treatment. Following pretreatment with 30 μM quercetin, lycopene, or M2, HUVEC cells were washed and resuspended with PBS, divided into seven aliquots in an equal volume, and heated individually at different temperatures (37°C–72 °C) for 5 min and then cooled at room temperature for 3 min. They were lysed with RIPA solution. Following centrifugation at 14,000g for 15 min at 4 °C, the supernatants were transferred to new tubes and stored at -80 °C until immunoblotting was performed.

2.8. SIRT1 enzymatic assay

The effects of quercetin, lycopene, and their combination on SIRT1 activity were assessed using the SIRT1/Sir2 Deacetylase Fluorometric (Human) Assay Kit (Abnova, Taiwan). According to the manufacturer's instructions, 5 μL of samples, fluoro-substrate peptide, NAD, and developer were added to microtiter plate wells and mix well. A total of 5 μL of recombinant SIRT1 was added to initiate reactions. The fluorescence intensity was read after 60 min using microtiter plate fluorometer with excitation at 340–360 nm and emission at 440–460 nm. The efficacy of samples on the SIRT1/Sir2 activity was the difference in fluorescence intensity between samples and solvent.

2.9. Fluorescence quenching

The fluorescence spectra (290–450 nm) of the interactions between phytochemicals and SIRT1 were collected on a spectrofluorimeter (Hitachi, F-7000, Japan). A total of 3 mL solution containing 9.6 μg SIRT1 was titrated by successively adding various amounts of quercetin, luteolin, lycopene, or lutein. The emission and excitation slit width was 10 nm, under the excitation wavelength of 280 nm, and a scanning rate of 1200 nm/min.

2.10. Evaluation of synergistic and antagonism effect

Flavonoid-carotenoid combinations are binary combinations in different ratios. Synergistic effects are commonly defined as the enhanced effects of the combinations than individual compounds. Antagonistic effects refer to the combined effects that are inferior to the individual ones (Chen et al., 2021b; Sunan et al., 2015). The chosen concentration of quercetin, luteolin, lycopene, lutein was 8 μM , which is an effective concentration in preventing H_2O_2 -induced oxidative damage according to our previous study (Chen et al., 2021a). As the concentration of individual ones and flavonoid-carotenoid combinations is equal, the synergistic effects refer to the stronger effects of combinations than the individuals ($p < 0.05$), and antagonistic effects refer to the weaker effects of combinations than the individuals ($p < 0.05$). This

evaluation method for synergism and antagonism was commonly adopted in cellular and animal experiments (Chen et al., 2021b; Hu et al., 2016; Li et al., 2019).

2.11. Statistical analysis

Statistical analysis was performed with IBM SPSS Statistics 20 software. Data are presented as mean \pm standard deviation (SD, $n \geq 3$). Significant differences between and within multiple groups were examined using one-way ANOVA with Duncan's test and $p < 0.05$ was considered statistically significant. The graphics were generated with GraphPad Prism 8.0 (GraphPad Software, San Diego, USA) and Origin-Pro 2019b (OriginLab Corporation, Northampton, MA, USA).

3. Results

3.1. Effects of various flavonoid-carotenoid combinations on H_2O_2 -induced ROS level production and Nox4 expression

Previously, the flavonoid-carotenoid combinations showed strong antioxidant activity in HUVEC cells, which may indicate the potent endothelial protective effects (Chen et al., 2021a). Further, 5 strong synergistic groups (M1 = lycopene: luteolin 1:5, M2 = lycopene: quercetin 1:5, M3 = lutein: luteolin 1:5, M4 = lutein: luteolin 5:1, M5 = lutein: quercetin 1:1, molar ratio), and one antagonistic group (M6 = lutein: quercetin 5:1) were selected to investigate the effects of the flavonoid-carotenoid combinations on ameliorating oxidative stress in HUVEC cells.

Flavonoids, carotenoids, and their combinations significantly reduced the ROS level compared to the H_2O_2 -treated group (Fig. 1A). M1-M5 showed significantly stronger effects than the individual compounds on inhibiting ROS levels, indicating synergistic effects. While M6 showed significantly weaker effects than the individual compounds on ROS inhibition, indicating significantly antagonistic effects. H_2O_2 treatment induced 2-fold Nox4 expression, while individual and combined phytochemical groups significantly reduced the Nox4 expression (Fig. 1B). M1, M2, and M3 showed synergistic effects on inhibiting the Nox4 expression, while M6 exhibited antagonism in reducing the Nox4 expression in a non-significant way. M2 showed the strongest synergism in suppressing the Nox4 expression, reducing 3.5-fold Nox4 expression compared to the H_2O_2 treatment. Another important NADPH oxidase, Nox2, was activated by H_2O_2 treatment as the expression of Nox2 increased around 1.4-fold. The expression of Nox2 was decreased by flavonoids, carotenoids, and flavonoid-carotenoid combinations, but no combinations showed significantly synergistic effects (Fig. S1A). It may indicate that flavonoid-carotenoid combinations showed interaction in Nox4 regulation other than Nox2 expression.

NADPH oxidases are one of the main sources of ROS *in vivo*. As indicated in Fig. S1B and Fig. S1C, ROS level increased with the increase of H_2O_2 concentration. Correspondently, the expression of Nox4 increased with the increase of H_2O_2 concentration, and showed a significant increase at 1500 μM compared to the control group. Therefore, inhibiting Nox4 activity may be critical to restoring the redox balance.

3.2. Involvement of NF- κ B signaling pathway in quercetin-lycopene combination-regulated Nox4 expression

Quercetin-lycopene combination M2 synergistically inhibited the ROS elevation. To explore the molecular mechanisms associated with the phenotypes observed in H_2O_2 -treated and M2-treated HUVEC cells, the mRNA expression profiles were examined by RNA sequencing (RNA-seq) analysis in HUVEC cells. The gene expression variation among control, H_2O_2 -treated, and M2-treated cells was presented in the heatmap (Fig. S2A). A total of 138 upregulated genes and 186 downregulated genes were identified in H_2O_2 treatment compared to the control group in HUVEC cells using the criterion of $q < 0.05$ and $|\log_2$

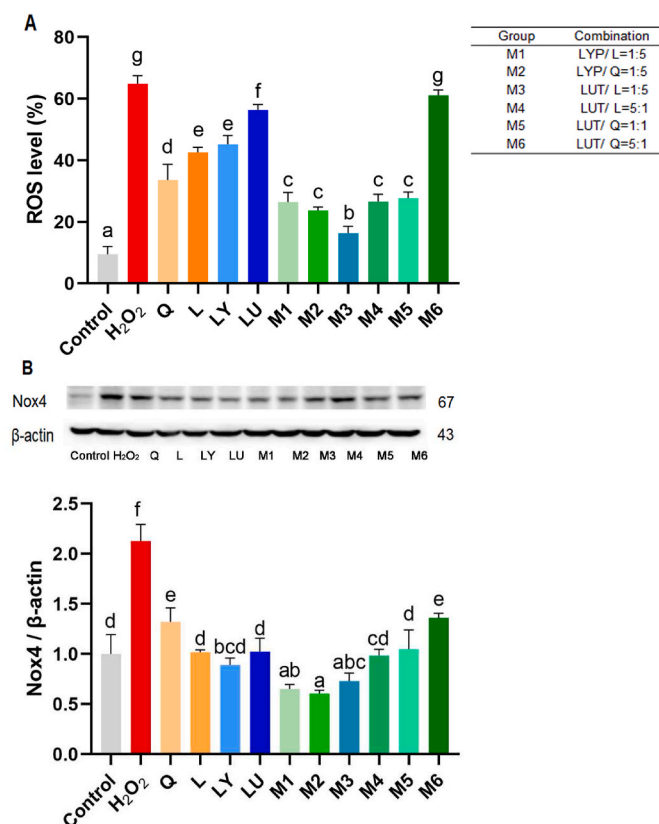


Fig. 1. Effects of flavonoid-carotenoid combinations on H₂O₂-induced ROS elevation and Nox4 expression. (A) ROS levels were reduced after being treated with individual flavonoid, carotenoid, or flavonoid-carotenoid combination. (B) The elevation of NADPH oxidase 4 (Nox4) expression induced by H₂O₂ was inhibited after being treated with individual flavonoid, carotenoid, or flavonoid-carotenoid combinations. n = 3 in each group. Different letters above the bar indicated a significant difference (p < 0.05) among groups. Q: quercetin; L: luteolin; LY: lycopene; LU: lutein; M1: LYP/L = 1:5; M2: LYP/Q = 1:5; M3: LUT/L = 1:5; M4: LUT/L = 5:1; M5: LUT/Q = 1:1; M6: LUT/Q = 5:1.

fold change|>1 (Fig. S2B). Compared with the H₂O₂-treated group, the M2-treated group downregulated 124 genes and upregulated 10 genes analyzed using the DEGseq database (>2-fold H₂O₂ treatment, q < 0.05, Fig. 2C).

Further, the biological pathways that were potentially altered by M2 treatment were analyzed using GO biological process analysis (GO_p). It showed specific downregulation in genes associated with the GO_p terms such as “inflammatory response”, “positive regulation of vascular endothelial growth factor production”, “positive regulation of transcription by RNA polymerase II”, and “skeletal muscle cell differentiation” (Fig. 2D). Interestingly, the most significant GO_p term for altered genes was “inflammatory response” (P = 2 × 10⁻⁸). This result implicated the potential modulation of the vascular inflammatory response by M2. According to the heatmap of enriched DEGs in the term “inflammatory response”, 16 genes were significantly altered by M2 in HUVEC cells, including one upregulated gene TICAM2, and 15 downregulated genes, such as PTGS2, PTGER3, C5AR1, NLRP3, IL1β, BCL-6. (Fig. 2E). Also, KEGG analysis revealed those DEGs were enriched in biological processes such as “IL-17 signaling pathway”, “C-type receptor signaling pathway”, “TNF signaling pathway”, which were related to the inflammatory response (Fig. S2C), and the enriched DEGs in the KEGG analysis of inflammatory-related terms are presented in the heatmap (Fig. S2D). These also implicated that M2 may regulate inflammatory genes to prevent oxidative stress in HUVEC cells. The NF-κB pathway was shown to play a critical role in the development of inflammation and vascular disorders (Ungvari et al., 2004). Gene set enrichment analysis (GSEA) of

RNA-seq revealed a significant enrichment of DEGs in the NF-κB pathway (Fig. 2F). A positive or negative normalized enrichment score (NES) indicated the increased or decreased expression in HUVEC cells. The enrichment in NF-κB signaling pathway-related genes was significantly downregulated in the M2 treatment group compared to that in the H₂O₂ treated group (NES = -1.70, p < 0.001).

To explore the synergistic effects of quercetin-lycopene combination and validate the RNA-seq results, the mRNA levels of 10 inflammatory-related genes downregulated by M2 were evaluated, including PTGS2, BCL6, IL-6, AO3, C5AR1, FOS, IL-1β, NFKBIZ, NLRP3, and SLC11A1. From the results, H₂O₂ treatment significantly induced the mRNA level of these genes, while quercetin, lycopene, and M2 treatment reduced their mRNA levels, except for NLRP3 and IL-1β (Fig. 2G and S3). PTGS2, which encoded COX-2 protein, was significantly reduced by M2 treatment than quercetin and lycopene. COX-2 is a cyclooxygenase that could induce inflammation, promote endothelial dysfunction, and be regulated by the transcription factor NF-κB (Kauppinen et al., 2013). M2 also showed a synergistic effect in regulating BCL6 mRNA level. These implicated that quercetin and lycopene could regulate some inflammatory-related genes synergistically. Considering that the NF-κB pathway is one of the major inflammatory pathways, the effects of quercetin, lycopene, and M2 on the expression of NF-κB p65, one of the critical roles in the activating of NF-κB transcriptional activity were further studied. It was shown that H₂O₂ treatment significantly activated p65 by increasing the phosphorylation of p65 (Fig. 2H). Quercetin and lycopene significantly reversed the activation of p65, and M2 showed a stronger effect on inhibiting phosphorylated p65 expression than the individual groups.

3.3. Quercetin and lycopene directly interacted with SIRT1 protein

SIRT1 is a deacetylase that plays an important role in regulating oxidative stress (Zhang et al., 2020). NF-κB was reported to be regulated by SIRT1 deacetylation to reduce oxidative stress and muscle loss (Kauppinen et al., 2013; Yeung et al., 2004). CETSA has been widely applied as a powerful method to assess ligand-protein binding effects by monitoring ligand-induced changes in the thermal stability of cellular proteins (Jafari et al., 2014). In this study, CETSA was performed to evaluate the effects of the quercetin-lycopene combination on SIRT1 stability. The interaction of quercetin, lycopene, and M2 with SIRT1 protein was studied. The band intensities of immunoblotting were quantified and plotted versus temperature (Fig. 3A). The abundance of SIRT1 was decreased with the increased temperatures, which implicated that the thermostability of endogenous SIRT1 could be monitored by this method. In the range from 37 °C to 47 °C, quercetin, lycopene, and M2 showed higher SIRT1 expression, suggesting ligand-dependent stabilization. The abundance of SIRT1 treated with quercetin or lycopene slumped after 47 °C, while the lysates treated with M2 did not significantly decrease till 57 °C. Also, the lysates treated with M2 showed a significantly higher abundance of SIRT1 than those treated with quercetin or lycopene at 52 °C. Hence, it was indicated that the quercetin-lycopene combination showed a stronger ability in stabilizing SIRT1 than the individual ones, which may underpin the molecular basis of the synergistic effects of M2 in SIRT1 expression.

The ability of the quercetin-lycopene combination to directly enhance SIRT1 deacetylation activity was determined through a SIRT1/Sir2 deacetylase fluorometric assay. Compared to the control group (which contains recombinant SIRT1), a positive value produced by samples (containing both recombinant SIRT1 and tested compounds) indicated the test compounds as activators, while a negative value implicated the test compounds as inhibitors. Quercetin enhanced SIRT1 activity and showed a dose-dependent tendency (Fig. S4A). Lycopene also increased SIRT1 activity in a dose-dependent manner (Fig. S4B). M2 showed a stronger enhancement in SIRT1 deacetylation activity than quercetin and lycopene at 8 μM (Fig. 3B). These results confirmed that quercetin, lycopene, and their combination could be used as SIRT1

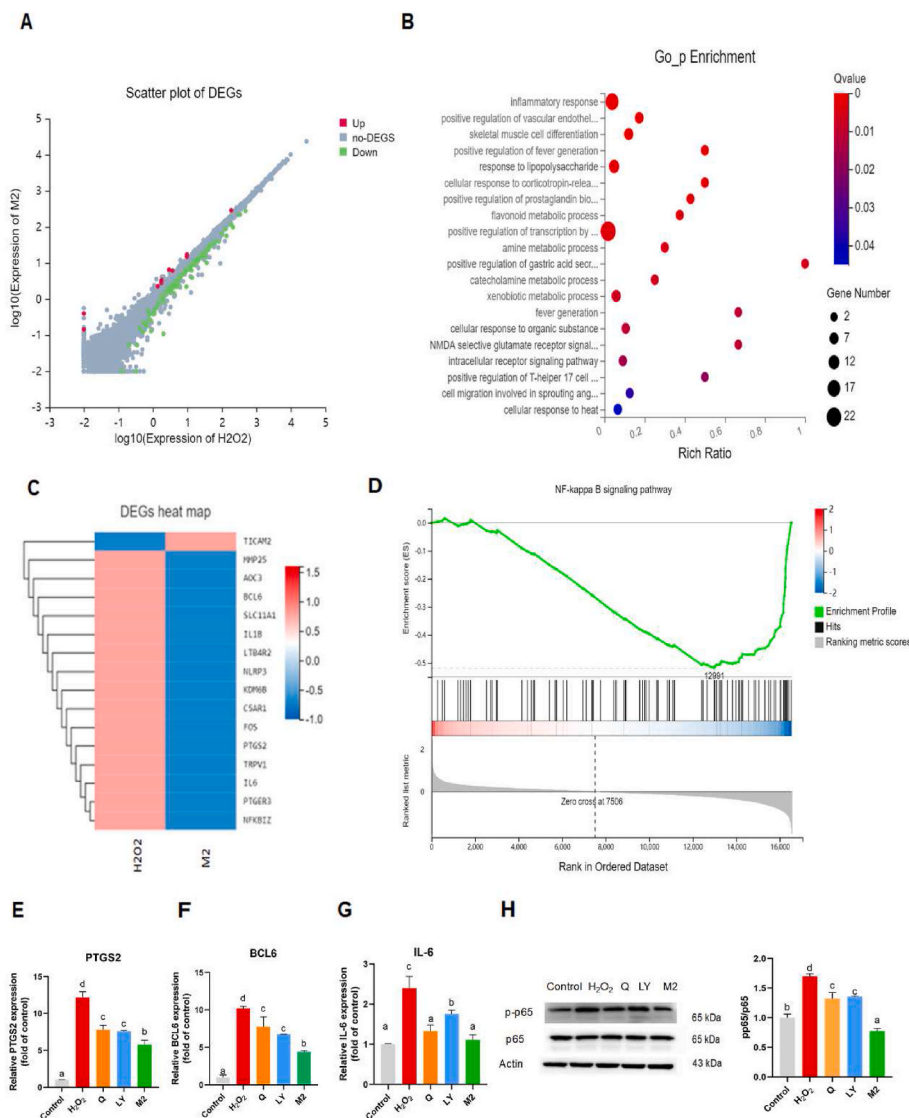


Fig. 2. Quercetin-lycopene combination suppressed H₂O₂-upregulated inflammatory-related gene expression. (A) Scatter plot of differentially expressed genes (DEG) between H₂O₂ and M2 treated group. M2: LYP: Q = 1:5. (B) GO enrichment analyses of DEGs between H₂O₂ treated group and M2 treated group. (C) Heatmap of enriched DEGs in the GO analysis term “Inflammatory response”. (D) Gene set enrichment analysis (GSEA) plots showing altered genes related to the NF-κB signaling pathway. The plots were based on the results from KEGG analysis of differentially expressed genes between H₂O₂ treated group and M2 group. NES, normalized enrichment score. FDR, false discovery rate. Green line indicates an enrichment profile, black vertical lines indicate hits, and gray vertical lines show ranking metric scores. (E–G) RT-qPCR analysis show the altered inflammatory genes by quercetin, lycopene, or M2. (H) Western blotting analysis of NF-κB p65 expression in HUVEC cells. n = 3 in each group. Different letters above the bar indicated a significant difference (*p* < 0.05) among groups. Q: quercetin; L: luteolin; LY: lycopene; LU: lutein; M2: LYP: Q = 1:5. (For interpretation of the references to colour in this figure legend, the reader is referred to the Web version of this article.)

activators.

In HUVEC cells, H₂O₂ significantly reduced the mRNA level of SIRT1 to around 38% (Fig. 3C), while lycopene significantly restored the SIRT1 mRNA level, and M2 increased around 4-fold of the SIRT1 mRNA level than lycopene, which indicated significant synergistic effects on inducing SIRT1 expression.

In addition, to verify the binding affinity of quercetin and lycopene with SIRT1, the fluorescence quenching assay was used (Dohare et al., 2018). As shown in Fig. 4C, a maximum fluorescence emission peak of SIRT1 was observed at 304 nm after being excited at 280 nm. The SIRT1 fluorescence was quenched due to the successive additions of quercetin, lycopene, or their combination M2 without any noticeable peak shift, indicating an interplay between these ligands and SIRT1. The Stern-Volmer equation was subsequently utilized to compare their interaction (Danesh et al., 2018). The Stern-Volmer plots presented good linearity in quercetin, lycopene, or M2 (Fig. 3D). K_{SV} is the Stern-Volmer dynamic quenching constant that showed quenching efficiency (Fig. 3E). M2 showed the strongest interplay with SIRT1, as the SIRT1-M2 possessed the highest K_{SV} value at 6.34 × 10⁴ L mol⁻¹. In addition, the K_{SV} value of SIRT1-lycopene was 6.10 × 10⁴ L mol⁻¹, which was higher than that of SIRT1-quercetin (5.11 × 10⁴ L mol⁻¹), suggesting that lycopene was more ready to interact with SIRT1 compared to quercetin. As shown in Table S2, quenching rate constant

K_q values of the quenching procedure (of 10¹² L mol⁻¹ s⁻¹ magnitude order) were higher than 2.0 × 10¹⁰ L mol⁻¹ s⁻¹, which is the quenching rate constant for maximum diffusion collision (Danesh et al., 2018). It was indicated that the effects of quercetin, lycopene, and M2 on the SIRT1 fluorescence quenching were due to the formation of a ground-state complex rather than a dynamic collision.

3.4. SIRT1-mediated inhibition of quercetin-lycopene combination on NF-κB and Nox4 expression

To explore the role of SIRT1 in regulating ROS level, 10 μM EX-527 were applied to HUVEC cells for 1 h to inhibit SIRT1 expression, which would not induce cytotoxicity (Figs. S5–6). The suppression of Nox4 and NF-κB p65 expressions by quercetin, lycopene, and M2 were abrogated by EX-527 (Fig. 4A–C). Correspondently, the inhibition of ROS elevation by quercetin, lycopene, and M2 was attenuated when pretreated with EX-527 (Fig. 4D). Diminished SIRT1 expression promoted the expression of Nox4 and activation of p65. These results indicated the regulating role of SIRT1 in inhibiting cellular ROS generation, and the quercetin-lycopene combination could inhibit ROS elevation through the SIRT1-Nox4 signaling pathway to prevent oxidative stress in HUVEC cells.

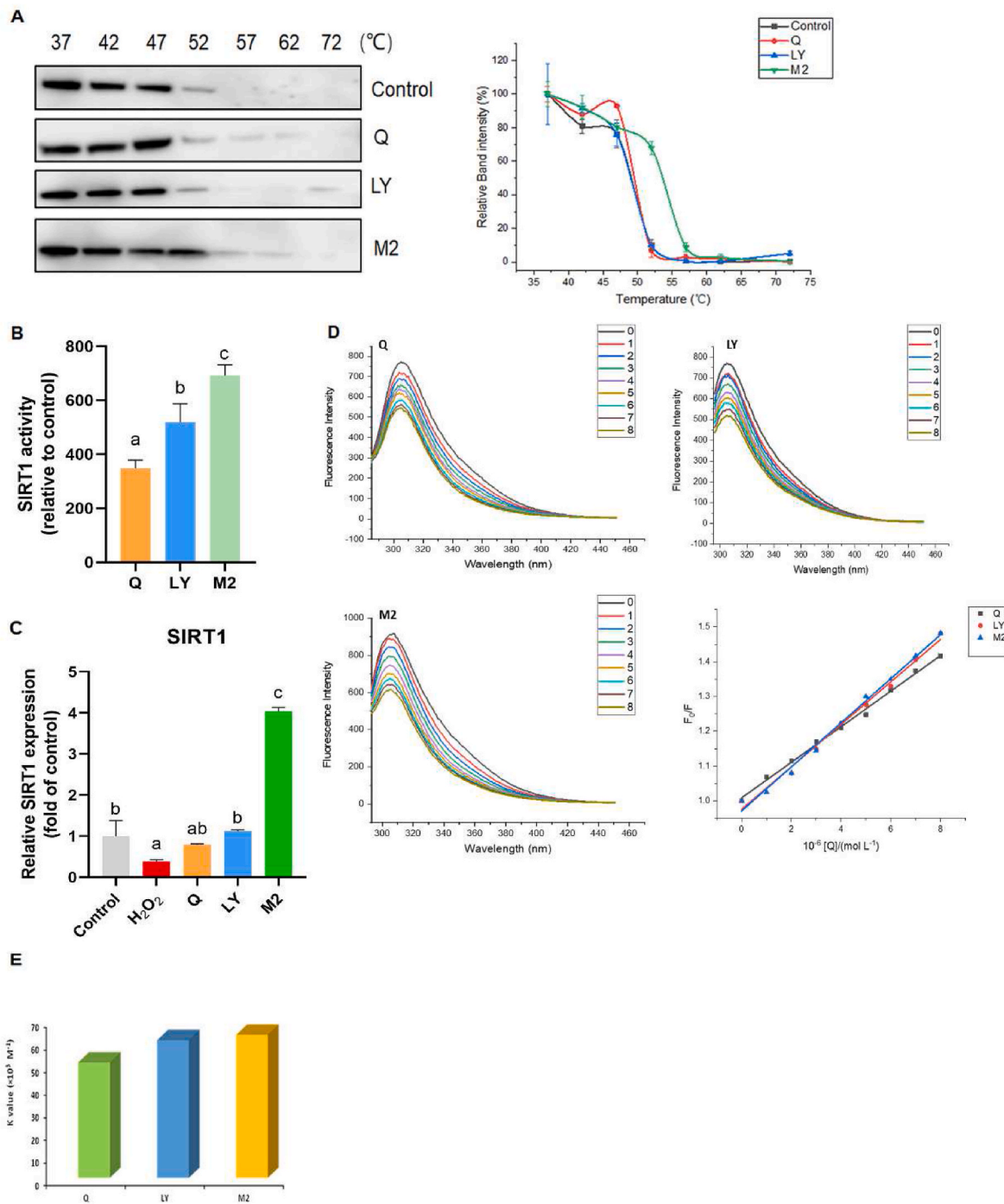


Fig. 3. Quercetin and lycopene directly interacted with human SIRT1 protein. (A) The thermostability of SIRT1 was increased by quercetin, lycopene, and M2. CETSA curves were built by plotting the intensity of the immunoblotting bands versus temperature. n = 3 in each group. Different letters above the bar indicated a significant difference ($p < 0.05$) among groups. (B) SIRT1 deacetylation activities were enhanced by quercetin, lycopene, and M2. (C) RT-qPCR analysis showed the up-regulated SIRT1 mRNA level by quercetin-lycopene combination in HUVEC cells. (D) Quenching of SIRT1 fluorescence by quercetin, lycopene, or M2 at different molar ratios. Lower right: the Stern-Volmer curves for estimating the binding constants (K values) of SIRT1 (pH 6.8, T = 311.15 K, $\lambda_{ex} = 280$ nm, $\lambda_{em} = 304$ nm). c (sirt1) = 0.6 $\mu\text{g}/\mu\text{L}$, c (Q), c (LY), c (M2) = 0–8 μM respectively. (E) K values (binding constants) of quercetin, lycopene, and M2.

4. Discussion

Oxidative stress is a critical event in the development of many CVDs such as atherosclerosis, hypertension, aging, and heart failure (Devasagayam et al., 2004). Here, the endothelial protective effects of the quercetin-lycopene combination by suppressing excessive ROS production were demonstrated in HUVEC cells. Flavonoid-carotenoid combinations, especially quercetin-lycopene combination (LYP: Q = 1:5),

interacted with deacetylase SIRT1 to inhibit NF- κ B p65 and Nox4 enzyme, downregulated inflammatory cytokines such as IL-6 and pro-inflammatory enzymes such as COX-2, and suppressed ROS elevation activated by H₂O₂.

Flavonoids and carotenoids have been reported to prevent various chronic diseases such as cardiovascular diseases by inhibiting excessive ROS production (Chen et al., 2020; Chen et al., 2021c; Hung et al., 2015). Especially, they could downregulate Nox4 to reduce intracellular

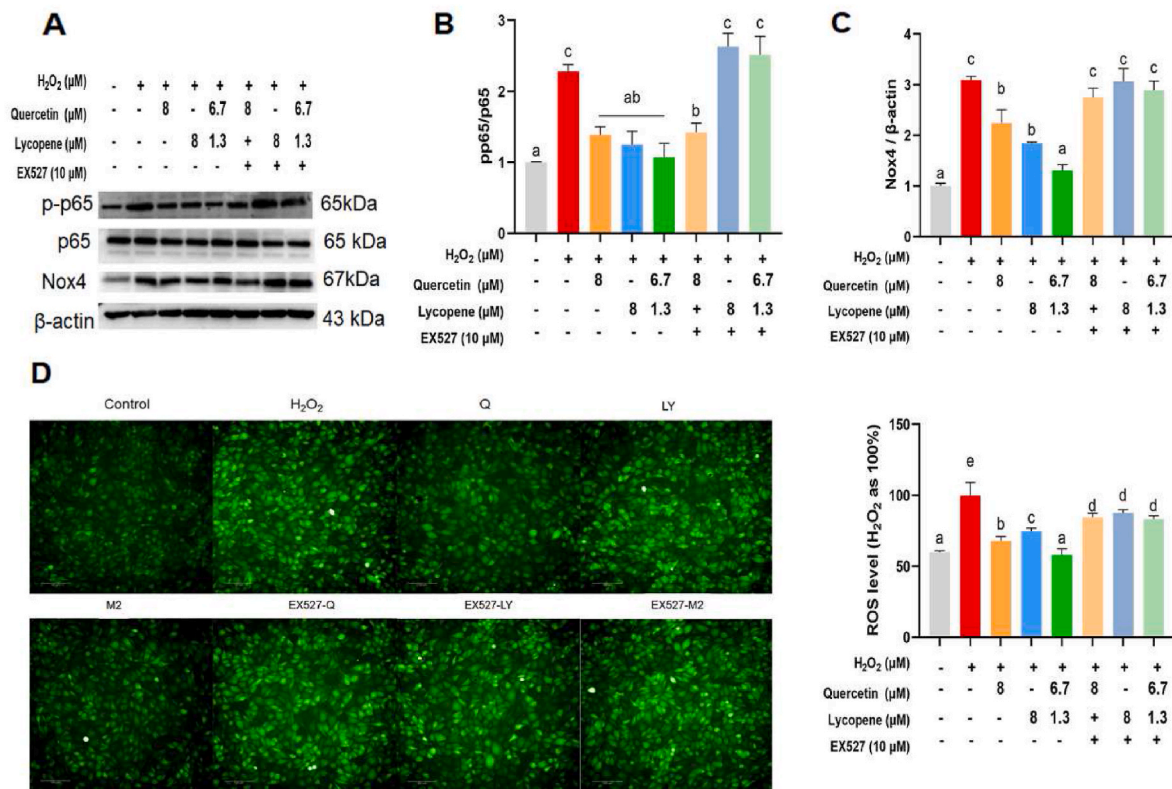


Fig. 4. SIRT1 inhibition altered the effects of quercetin-lycopen combination on NF-κB p65 and Nox4 expressions, as well as ROS level. (A) Representative immunoblots of NF-κB p65 and Nox4 expression after being treated with or without SIRT1 inhibitor EX-527 in HUVEC cells. Cells were treated with or without 10 μM EX-527 for 1 h, and treated with 8 μM quercetin, lycopene, or M2 for 12 h, and further treated with or without 1500 μM H₂O₂ for 1 h. (B) The expression of NF-κB p65 in HUVEC cells. (C) The expression of Nox4 in HUVEC cells. (D) ROS level increased after being treated with SIRT1 inhibitor EX-527. n = 3 in each group. Different letters above the bar indicated a significant difference ($p < 0.05$) among groups.

ROS levels and prevent oxidative stress-induced diseases (Hung et al., 2015; Zhou et al., 2017). In addition, Nox2 and Nox4 are highly expressed in the heart and are critical to the development of cardiomyocytes, especially Nox4, distinguished from the other Nox isoforms because of their high level in cardiovascular tissues (Maejima et al., 2011). Nox4 may therefore be more susceptible to stress factors, such as H₂O₂-induced oxidative stress than Nox2 (Chen et al., 2012). Correspondently, we found that the expression of Nox4 was elevated around 2-fold and Nox2 expression was increased around 1.4- fold by H₂O₂. While flavonoids, carotenoids, and their combinations significantly inhibited the expression of Nox2 and Nox4. Thus, flavonoid-carotenoid combinations may regulate ROS levels in a Nox4-dependent manner.

Quercetin-lycopen combination altered 134 genes on the deregulated signaling pathways induced by H₂O₂, especially those genes enriched in inflammatory-related pathways, such as the NF-κB signaling pathway, which was identified by RNA-sequencing analysis. Hou et al. (2019) also reported that 4 h of H₂O₂ treatment induced DEGs enriched in inflammation, immune response, and apoptosis signaling pathways, especially those enriched in NF-κB and TNF signaling in Caco-2 cells. Inflammatory cytokines such as IL1-β, IL-6, IL-2, NLRP3, and related enzymes such as COX-2 were reported to activate transcription factor NF-κB triggering inflammation response and vascular dysfunction (Rodríguez-Mañas et al., 2009; Yu and Chung, 2006). Such inflammatory responses induced ROS overproduction and then triggered oxidative stress (Crowley, 2014). In our study, the activated inflammatory genes by H₂O₂ could result from the activation of inflammatory signaling pathways, which further exacerbated oxidative stress, which was ameliorated by the quercetin-lycopen combination.

SIRT1 has been reported to confer endothelial protection through

ameliorating oxidative stress, and be downregulated by oxidative stress factors such as H₂O₂, hypoxia, hyperglycemia et al. (Chen et al., 2018; Crowley, 2014; Rodríguez-Mañas et al., 2009). Evidence piled up that quercetin, luteolin, lycopene, and lutein could prevent oxidative stress, endothelial dysfunction, and aging via up-regulating SIRT1 (Balcerczyk et al., 2014; Hung et al., 2015; Luvizotto et al., 2015). However, the interaction between them is not clear. In this study, we demonstrated the interaction of quercetin and lycopene with SIRT1 for the first time, by direct interaction, and changes in SIRT1 thermo-stabilization. Our results showed that quercetin-lycopen combination M2 increased the thermostability of SIRT1 determined by CETSA, showed higher efficiency in boosting SIRT1 deacetylation, and a stronger affinity to SIRT1 in fluorescence quenching assay. The changes in the stability of SIRT1 may be a direct result of drug binding, but also could result from downstream effects such as modulation of cell signaling, and metabolism induced by the small compounds (Danesh et al., 2018). Previous studies reported that the modifications on cysteine residues and other modifications such as glutathionylation and sulfenylation could change the stability of the protein, which was observed by the previous CETSA study (He et al., 2015). Thus, the CETSA results may also indicate a possible change in deacetylase activities of SIRT1 by quercetin and M2. The activation of SIRT1 depended on a direct combination with SIRT1 and further activating SIRT1-catalyzed deacetylation, or improving the stability of SIRT1 (Gertz et al., 2012; Lakshminarasimhan et al., 2013). We found that quercetin and lycopene synergistically increase the deacetylase activities of SIRT1, as well as the mRNA level of SIRT1.

Sirt1-mediated deacetylation was reported to regulate the NF-κB pathway in vascular smooth muscle cells and other models (Chen et al., 2016; Kauppinen et al., 2013). NF-κB transcription activity was suppressed by SIRT1 binding and deacetylating subunit p65 (Salminen

et al., 2008; Yeung et al., 2004), which altered redox balance and reduced muscle wasting in tumor-bearing mice (Dasgupta et al., 2020). The expression of NF- κ B p65 was induced by H₂O₂, while inhibited by quercetin-lycopene combination in HUVEC cells, with SIRT1 involved. Nox4, distinguished from the other Nox isoforms by its high level in cardiovascular tissues, plays a critical role in endothelial oxidative stress (Maejima et al., 2011). Flavonoids and carotenoids could downregulate Nox4 to reduce intracellular ROS levels and prevent oxidative stress-induced diseases (Hung et al., 2015; Zhou et al., 2017). SIRT1 can regulate oxidative stress and prevent cancer cachexia in skeletal muscles via Nox4 (Dasgupta et al., 2020). The inhibition of SIRT1 induced endothelial dysfunction via upregulation of the NADPH oxidase subunits, p22phox and Nox4, resulting in an increased vascular O₂⁻ production (Zarzuelo et al., 2013). We found that inhibition of SIRT1 abolished the suppression of Nox4 and ROS levels by the quercetin-lycopene combination. In addition, Nox4 was also stimulated by NF- κ B in vascular smooth cells and other models (Lu et al., 2010; Ryu et al., 2007). The NF- κ B subunits p65 and p50 activated Nox4 promoter activity, while the inhibition of NF- κ B p50 or p65 decreased hypoxia-driven Nox4 promoter activity in human pulmonary artery smooth muscle cells (Lu et al., 2010). Taken together, these results indicated the important role of SIRT1 in inhibiting ROS generation. That is to say, the quercetin-lycopene combination could inhibit ROS elevation through the SIRT1-Nox4 signaling pathway.

Overall, this study demonstrated that flavonoid-carotenoid combination, especially quercetin-lycopene combination, interacts with SIRT1 to suppress inflammation and Nox4 expression, reduced ROS production, and prevent oxidative stress in HUVEC cells. Therefore, choosing a balanced diet containing both flavonoids and carotenoids is beneficial for preventing vascular disorders and related cardiovascular diseases.

CRedit authorship contribution statement

Xuan Chen: Formal analysis, Methodology, Writing – original draft. **Liufeng Zheng:** Methodology, Formal analysis. **Bing Zhang:** Methodology. **Zeyuan Deng:** Conceptualization, Supervision, Project administration. **Hongyan Li:** Conceptualization, Supervision, Funding acquisition, Writing – review & editing.

Declaration of competing interest

The authors declare that they have no known competing financial interests or personal relationships that could have appeared to influence the work reported in this paper.

Acknowledgment

This research was supported by the National Natural Science Foundations of China (Grant No.: 31972970 and 21964012) and Central Government Guide Local Special Fund Project for Scientific and Technological Development of Jiangxi Province (20221ZDD02001).

Appendix A. Supplementary data

Supplementary data to this article can be found online at <https://doi.org/10.1016/j.crfs.2022.10.018>.

References

Balcerczyk, A., Gajewska, A., Macierzyńska-Piotrowska, E., Pawelczyk, T., Bartosz, G., Szymraj, J., 2014. Enhanced antioxidant capacity and anti-ageing biomarkers after diet micronutrient supplementation. *Molecules* 19 (9), 14794–14808.

Chen, A., Chen, Z., Xia, Y., Lu, D., Yang, X., Sun, A., Zou, Y., Qian, J., Ge, J., 2018. Liraglutide attenuates NLRP3 inflammasome-dependent pyroptosis via regulating SIRT1/NOX4/ROS pathway in H9c2 cells. *Biochem. Biophys. Res. Commun.* 499 (2), 267–272.

Chen, X., Deng, Z., Zheng, L., Zhang, B., Luo, T., Li, H., 2021a. Interaction between flavonoids and carotenoids on ameliorating oxidative stress and cellular uptake in different cells. *Foods* 10 (12).

Chen, F., Haigh, S., Barman, S., Fulton, D.J., 2012. From form to function: the role of Nox4 in the cardiovascular system. *Front. Physiol.* 3, 412.

Chen, H.I., Hu, W.S., Hung, M.Y., Ou, H.C., Huang, S.H., Hsu, P.T., Day, C.H., Lin, K.H., Viswanatha, V.P., Kuo, W.W., Huang, C.Y., 2020. Protective effects of luteolin against oxidative stress and mitochondrial dysfunction in endothelial cells. *Nutr. Metabol. Cardiovasc. Dis.* 30 (6), 1032–1043.

Chen, X., Li, H., Zhang, B., Deng, Z., 2021b. The synergistic and antagonistic antioxidant interactions of dietary phytochemical combinations. *Crit. Rev. Food Sci. Nutr.* 1–20.

Chen, Y., Liu, H., Zhang, H., Liu, E., Xu, C.B., Su, X., 2016. The sirt1/NF- κ B signaling pathway is involved in regulation of endothelin type B receptors mediated by homocysteine in vascular smooth muscle cells. *Biomed. Pharmacother.* 84, 1979–1985.

Chen, Y., Wang, L., Huang, S., Ke, J., Wang, Q., Zhou, Z., Chang, W., 2021c. Lutein attenuates angiotensin II-induced cardiac remodeling by inhibiting AP-1/IL-11 signaling. *Redox Biol.* 44, 102020.

Crowley, S.D., 2014. The cooperative roles of inflammation and oxidative stress in the pathogenesis of hypertension. *Antioxidants Redox Signal.* 20 (1), 102–120.

D’Oria, R., Schipani, R., Leonardini, A., Natalicchio, A., Perrini, S., Cignarelli, A., Laviola, L., Giorgino, F., 2020. The role of oxidative stress in cardiac disease: from physiological response to injury factor. *2020 Oxid. Med. Cell. Longev.*, 5732956.

Danesh, N., Navaei Sedighi, Z., Beigoli, S., Sharifi-Rad, A., Saberi, M.R., Chamani, J., 2018. Determining the binding site and binding affinity of estradiol to human serum albumin and holo-transferrin: fluorescence spectroscopic, isothermal titration calorimetry and molecular modeling approaches. *J. Biomol. Struct. Dyn.* 36 (7), 1747–1763.

Dasgupta, A., Shukla, S.K., Vernucci, E., King, R.J., Abrego, J., Mulder, S.E., Mullen, N.J., Graves, G., Buettner, K., Thakur, R., Murthy, D., Attri, K.S., Wang, D., Chaika, N.V., Pacheco, C.G., Rai, I., Engle, D.D., Grandgenett, P.M., Punsoni, M., Reames, B.N., Teoh-Fitzgerald, M., Oberley-Deegan, R., Yu, F., Klute, K.A., Hollingsworth, M.A., Zimmerman, M.C., Mehla, K., Sadoshima, J., Tuveson, D.A., Singh, P.K., 2020. SIRT1-NOX4 signaling axis regulates cancer cachexia. *J. Exp. Med.* 217 (7).

Devasagayam, T.P., Tilak, J.C., Boloor, K.K., Sane, K.S., Ghaskadbi, S.S., Lele, R.D., 2004. Free radicals and antioxidants in human health: current status and future prospects. *J. Assoc. Phys. India* 52, 794–804.

Dohare, N., Khan, A.B., Maurya, N., Thakur, S., Athar, F., Singh, P., Patel, R., 2018. An insight into the binding of aceclofenac with bovine serum albumin at physiological condition: a spectroscopic and computational approach. *J. Biomol. Struct. Dyn.* 36 (2), 398–406.

Gertz, M., Nguyen, G.T., Fischer, F., Suenkel, B., Schlicker, C., Fränzel, B., Tomaszewski, J., Aladini, F., Becker, C., Wolters, D., Steegborn, C., 2012. A molecular mechanism for direct sirtuin activation by resveratrol. *PLoS One* 7 (11), e49761.

Goligorsky, M.S., 2005. Endothelial cell dysfunction: can’t live with it, how to live without it. *Am. J. Physiol. Ren. Physiol.* 288 (5), F871–F880.

He, N., Zhu, X., He, W., Zhao, S., Zhao, W., Zhu, C., 2015. Resveratrol inhibits the hydrogen peroxide-induced apoptosis via Sirt 1 activation in osteoblast cells. *Biosci. Biotechnol. Biochem.* 79 (11), 1779–1786.

Hou, Y., Li, X., Liu, X., Zhang, Y., Zhang, W., Man, C., Jiang, Y., 2019. Transcriptomic responses of Caco-2 cells to Lactobacillus rhamnosus GG and Lactobacillus plantarum J26 against oxidative stress. *J. Dairy Sci.* 102 (9), 7684–7696.

Hu, T.X., Wei, G., Xi, M.M., Yan, J.J., Wu, X.X., Wang, Y.H., Zhu, Y.R., Wang, C., Wen, A. D., 2016. Synergistic cardioprotective effects of Danshen and hydroxysafflower yellow A against myocardial ischemia-reperfusion injury are mediated through the Akt/Nrf2/HO-1 pathway. *Int. J. Mol. Med.* 38 (1), 83–94.

Hung, C.H., Chan, S.H., Chu, P.M., Tsai, K.L., 2015. Quercetin is a potent anti-atherosclerotic compound by activation of SIRT1 signaling under oxLDL stimulation. *Mol. Nutr. Food Res.* 59 (10), 1905–1917.

Jafari, R., Almqvist, H., Axelsson, H., Ignatushchenko, M., Lundbäck, T., Nordlund, P., Martinez Molina, D., 2014. The cellular thermal shift assay for evaluating drug target interactions in cells. *Nat. Protoc.* 9 (9), 2100–2122.

Jhou, B.Y., Song, T.Y., Lee, I., Hu, M.L., Yang, N.C., 2017. Lycopene inhibits metastasis of human liver adenocarcinoma SK-Hep-1 cells by downregulation of NADPH oxidase 4 protein expression. *J. Agric. Food Chem.* 65 (32), 6893–6903.

Kaulmann, A., Andre, C.M., Schneider, Y.J., Hoffmann, L., Bohn, T., 2016. Carotenoid and polyphenol bioaccessibility and cellular uptake from plum and cabbage varieties. *Food Chem.* 197 (Pt A), 325–332.

Kauppinen, A., Suuronen, T., Ojala, J., Kaarniranta, K., Salminen, A., 2013. Antagonistic crosstalk between NF- κ B and SIRT1 in the regulation of inflammation and metabolic disorders. *Cell. Signal.* 25 (10), 1939–1948.

Kim, D., Langmead, B., Salzberg, S.L., 2015. HISAT: a fast spliced aligner with low memory requirements. *Nat. Methods* 12 (4), 357–360.

Kim, J.Y., Paik, J.K., Kim, O.Y., Park, H.W., Lee, J.H., Jang, Y., Lee, J.H., 2011. Effects of lycopene supplementation on oxidative stress and markers of endothelial function in healthy men. *Atherosclerosis* 215 (1), 189–195.

Lakshminarasimhan, M., Curth, U., Moniot, S., Mosalaganti, S., Raunser, S., Steegborn, C., 2013. Molecular architecture of the human protein deacetylase Sirt1 and its regulation by AROS and resveratrol. *Biosci. Rep.* 33 (3).

Langmead, B., Salzberg, S.L., 2012. Fast gapped-read alignment with Bowtie 2. *Nat. Methods* 9 (4), 357–359.

Lassègue, B., Griendling, K.K., 2010. NADPH oxidases: functions and pathologies in the vasculature. *Arterioscler. Thromb. Vasc. Biol.* 30 (4), 653–661.

Li, B., Dewey, C.N., 2011. RSEM: accurate transcript quantification from RNA-Seq data with or without a reference genome. *BMC Bioinf.* 12, 323.

- Li, W.W., Wang, T.Y., Cao, B., Liu, B., Rong, Y.M., Wang, J.J., Wei, F., Wei, L.Q., Chen, H., Liu, Y.X., 2019. Synergistic protection of matrine and lycopene against lipopolysaccharide-induced acute lung injury in mice. *Mol. Med. Rep.* 20 (1), 455–462.
- Lu, X., Murphy, T.C., Nanes, M.S., Hart, C.M., 2010. PPAR γ regulates hypoxia-induced Nox4 expression in human pulmonary artery smooth muscle cells through NF- κ B. *Am. J. Physiol. Lung Cell Mol. Physiol.* 299 (4), L559–L566.
- Luvizotto, R.A., Nascimento, A.F., Miranda, N.C., Wang, X.D., Ferreira, A.L., 2015. Lycopene-rich tomato oleoresin modulates plasma adiponectin concentration and mRNA levels of adiponectin, SIRT1, and FoxO1 in adipose tissue of obese rats. *Hum. Exp. Toxicol.* 34 (6), 612–619.
- Maejima, Y., Kuroda, J., Matsushima, S., Ago, T., Sadoshima, J., 2011. Regulation of myocardial growth and death by NADPH oxidase. *J. Mol. Cell. Cardiol.* 50 (3), 408–416.
- Pan, Y., Deng, Z.-Y., Chen, X., Zhang, B., Fan, Y., Li, H., 2021. Synergistic antioxidant effects of phenolic acids and carotenes on H₂O₂-induced H9c2 cells: role of cell membrane transporters. *Food Chem.* 341.
- Pan, Y., Deng, Z.-y., Zheng, S.-l., Chen, X., Zhang, B., Li, H., 2018. Daily dietary antioxidant interactions are due to not only the quantity but also the ratios of hydrophilic and lipophilic phytochemicals. *J. Agric. Food Chem.* 66 (34), 9107–9120.
- Phan, M.A.T., Bucknall, M.P., Arcot, J., 2019. Interferences of anthocyanins with the uptake of lycopene in Caco-2 cells, and their interactive effects on anti-oxidation and anti-inflammation in vitro and ex vivo. *Food Chem.* 276, 402–409.
- Potente, M., Ghaeni, L., Baldessari, D., Mostoslavsky, R., Rossig, L., Dequiedt, F., Haendeler, J., Mione, M., Dejana, E., Alt, F.W., Zeiher, A.M., Dimmeler, S., 2007. SIRT1 controls endothelial angiogenic functions during vascular growth. *Genes Dev.* 21 (20), 2644–2658.
- Rodríguez-Mañas, L., El-Assar, M., Vallejo, S., López-Dóriga, P., Solís, J., Petidier, R., Montes, M., Nevado, J., Castro, M., Gómez-Guerrero, C., Peiró, C., Sánchez-Ferrer, C. F., 2009. Endothelial dysfunction in aged humans is related with oxidative stress and vascular inflammation. *Aging Cell* 8 (3), 226–238.
- Ryu, J., Lee, C.W., Shin, J.A., Park, C.S., Kim, J.J., Park, S.J., Han, K.H., 2007. FcγRIIIa mediates C-reactive protein-induced inflammatory responses of human vascular smooth muscle cells by activating NADPH oxidase 4. *Cardiovasc. Res.* 75 (3), 555–565.
- Salminen, A., Huuskonen, J., Ojala, J., Kauppinen, A., Kaarniranta, K., Suuronen, T., 2008. Activation of innate immunity system during aging: NF- κ B signaling is the molecular culprit of inflamm-aging. *Ageing Res. Rev.* 7 (2), 83–105.
- Santilli, F., D'Ardes, D., Davì, G., 2015. Oxidative stress in chronic vascular disease: from prediction to prevention. *Vasc. Pharmacol.* 74, 23–37.
- Schilder, Y.D., Heiss, E.H., Schachner, D., Ziegler, J., Reznicek, G., Sorescu, D., Dirsch, V. M., 2009. NADPH oxidases 1 and 4 mediate cellular senescence induced by resveratrol in human endothelial cells. *Free Radic. Biol. Med.* 46 (12), 1598–1606.
- Seals, D.R., Jablonski, K.L., Donato, A.J., 2011. Aging and vascular endothelial function in humans. *Clin. Sci. (Lond.)* 120 (9), 357–375.
- Shang, Z., Li, M., Zhang, W., Cai, S., Hu, X., Yi, J., 2022. Analysis of phenolic compounds in pickled chayote and their effects on antioxidant activities and cell protection. *Food Res. Int.* 157, 111325.
- Sinigalli, C., Faraoane, I., Vassallo, A., Caddeo, C., Bisaccia, F., Armentano, M.F., Milella, L., Ostuni, A., 2020. Phytochemical profile of capsicum annum L. Cv senise, incorporation into liposomes, and evaluation of cellular antioxidant activity. *Antioxidants* 9 (5).
- Sunan, W., Fan, Z., F. M.M., 2015. Synergistic interaction of sumac and raspberry mixtures in their antioxidant capacities and selective cytotoxicity against cancerous cells. *J. Med. Food* 18 (3), 345–353.
- Ungvari, Z., Csiszar, A., Kaley, G., 2004. Vascular inflammation in aging. *Herz* 29 (8), 733–740.
- Xiao, N., Mei, F., Sun, Y., Pan, G., Liu, B., Liu, K., 2014. Quercetin, luteolin, and epigallocatechin gallate promote glucose disposal in adipocytes with regulation of AMP-activated kinase and/or sirtuin 1 activity. *Planta Med.* 80 (12), 993–1000.
- Yeung, F., Hoberg, J.E., Ramsey, C.S., Keller, M.D., Jones, D.R., Frye, R.A., Mayo, M.W., 2004. Modulation of NF- κ B-dependent transcription and cell survival by the SIRT1 deacetylase. *EMBO J.* 23 (12), 2369–2380.
- Yu, B.P., Chung, H.Y., 2006. Adaptive mechanisms to oxidative stress during aging. *Mech. Ageing Dev.* 127 (5), 436–443.
- Yu, J., Auwerx, J., 2010. Protein deacetylation by SIRT1: an emerging key post-translational modification in metabolic regulation. *Pharmacol. Res.* 62 (1), 35–41.
- Yu, Y., Li, Z., Cao, G., Huang, S., Yang, H., 2019. Bamboo leaf flavonoids extracts alleviate oxidative stress in HepG2 cells via naturally modulating reactive oxygen species production and nrf2-mediated antioxidant defense responses. *J. Food Sci.* 84 (6), 1609–1620.
- Zarzuelo, M.J., López-Sepúlveda, R., Sánchez, M., Romero, M., Gómez-Guzmán, M., Ungvary, Z., Pérez-Vizcaíno, F., Jiménez, R., Duarte, J., 2013. SIRT1 inhibits NADPH oxidase activation and protects endothelial function in the rat aorta: implications for vascular aging. *Biochem. Pharmacol.* 85 (9), 1288–1296.
- Zhang, H., Tsao, R., 2016. Dietary polyphenols, oxidative stress and antioxidant and anti-inflammatory effects. *Curr. Opin. Food Sci.* 8, 33–42.
- Zhang, W., Huang, Q., Zeng, Z., Wu, J., Zhang, Y., Chen, Z., 2017. Sirt1 inhibits oxidative stress in vascular endothelial cells, 2017 *Oxid. Med. Cell. Longev.*, 7543973
- Zhang, X., Yu, Y., Lei, H., Cai, Y., Shen, J., Zhu, P., He, Q., Zhao, M., 2020. The nrf-2/HO-1 signaling Axis: a ray of hope in cardiovascular diseases, 2020 *Cardiol. Res. Pract.*, 5695723
- Zhang, Y., Cao, X., Zhu, W., Liu, Z., Liu, H., Zhou, Y., Cao, Y., Liu, C., Xie, Y., 2016. Resveratrol enhances autophagic flux and promotes ox-LDL degradation in HUVECs via upregulation of SIRT1, 2016 *Oxid. Med. Cell. Longev.*, 7589813
- Zheng, S., Deng, Z., Chen, F., Zheng, L., Pan, Y., Xing, Q., Tsao, R., Li, H., 2020. Synergistic antioxidant effects of petunidin and lycopene in H9c2 cells submitted to hydrogen peroxide: role of Akt/Nrf2 pathway. *J. Food Sci.* 85 (6), 1752–1763.